Plagioclase zoning in mid-Pleistocene lavas from the Seguam volcanic center, central Aleutian arc, Alaska

Bradley S. Singer

Department of Geological Sciences, Southern Methodist University, Dallas, Texas 75275, U.S.A.

Thomas H. Pearce, Angela M. Kolisnik

Department of Geological Sciences, Queen's University, Kingston, Ontario K7L 3N6, Canada

James D. Myers

Department of Geology and Geophysics, University of Wyoming, Laramie, Wyoming 82071, U.S.A.

Abstract

Nomarski and laser interferometry have been used to characterize plagioclase zoning in lavas ranging in composition from basalt to rhyodacite erupted at the Seguam volcanic center. This is the first application of these techniques to lavas that are related by closed-system crystal fractionation. Phenocrysts of An_{70-94} plagioclase in the basalts and basaltic andesites contain patchy-zoned cores mantled by sieve-textured zones rich in melt and fluid inclusions that alternate with euhedral oscillatory zones. Rarely, plagioclase cores are resorbed. Despite this complexity, no compositional shifts accompany these textural transitions. Andesites, dacites, and rhyodacites contain simpler phenocrysts with unzoned or oscillatory zoned cores of An_{40-70} surrounded by euhedral oscillatory zones. Initially euhedral zones are commonly rounded with compositional shifts of <5 mol% An accompanying these truncations. A less abundant population of crystals in the silicic lavas contain sieve-textured An_{80-92} cores overgrown by An_{40-70} euhedral oscillatory zones. Except for these xenocrysts, there exists a progressive decrease in An content with increasing bulk-rock SiO_2.

The lack of large amplitude ($\Delta 10-30$ mol% An) discontinuities or reverse zoning indicates a minor role for magma mixing. The sieve-textured zones probably reflect rapid growth, which trapped melt and volatiles during episodic decompression of the mafic magmas. Truncated zones in plagioclase of the silicic lavas may reflect repeated heating of crystals retained in convecting magma. Magma chambers beneath Seguam erupted frequently enough to limit convective recycling and plagioclase retention, resulting in phenocrysts with little or no compositional zoning. This type of dynamics contrasts with two other types of systems. In one, plagioclase retention and recycling is important; they increase the residence time of crystals in evolving magmas and produce continuous normal zoning from calcic cores to progressively more sodic mantles and rims. A third type of system is dominated by magma mixing, and plagioclase shows pronounced compositional and textural discontinuities. Reentrainment of crystals from cumulate mush zones along chamber walls explains the calcic-cored xenocrysts in the silicic lavas at Seguam and is probably common in each type of system. Because the rheological properties of magmas in these systems are similar, the contrasts in dynamics reflect differences in the rates of cooling, replenishment, and eruption of crustal magma chambers.

Introduction

Plagioclase zoning has received a great deal of attention because it records physical and chemical changes in the magmatic liquids from which the crystals grow (e.g., Vance, 1965; Wiebe, 1968; Loomis and Welber, 1982; Pearce et al., 1987a; Blundy and Shimizu, 1991). Experimental investigations have examined the effects of cooling and quenching (Lofgren, 1974), thermal and compositional disequilibrium produced by magma mixing (Lofgren and Norris, 1981; Tsuchiyama, 1985), and rapid isothermal decompression (Nelson and Montana, 1989, 1992) on plagioclase zoning. These experiments have produced dissolution, reaction, and growth textures and compositional zoning similar to those common in natural samples, and provide a basis for interpreting magma dynamics from plagioclase zoning.

Nomarski differential interference contrast microscopy (NDIC) and narrow fringe laser interference microscopy (NFLIM) offer resolution of remarkably fine-scale textural and compositional features of plagioclase zoning (Anderson, 1983; Pearce et al., 1987b; Pearce and Kolisnik,

TABLE 1. Whole rock major-element compositions, modal abundances, and rheological properties of Turf Point Formation lavas

Sample Rock type		B87-57 dike	J87-79 flow	B87-9 flow	B87-49 flow	B87-50 flow	87-67 flow	B87-56 flow
SiO_2		50.5	50.7	55.1	58.3	62.7	67.5	71.0
TiO_2		0.66	0.72	0.81	1.14	0.92	0.91	0.63
Al_2O_3		20.2	19.3	17.6	15.9	15.8	14.8	15.1
Fe_2O_3		6.57	2.06	2.72	1.72	1.49	1.24	1.73
FeO		1.24	5.97	5.52	8.81	4.84	3.72	2.25
MnO		0.13	0.15	0.15	0.17	0.14	0.14	0.11
MgO		5.20	6.02	5.49	3.29	2.39	1.27	0.73
CaO		11.5	11.3	9.66	7.33	5.49	3.63	2.62
Na_2O		2.15	2.18	2.73	3.59	4.07	4.75	4.87
K_2O		0.28	0.27	0.61	0.84	1.42	1.79	2.12
P_2O_5		0.12	0.13	0.14	0.18	0.22	0.27	0.15
LOI		0.29	−0.16	−0.32	−0.10	0.05	−0.18	−0.07
Total		98.87	98.68	100.28	101.15	99.45	99.86	101.22
Modal percentages of phenocrysts (>0.03 mm)								
Plag		25.7	42.1	22.3	3.1	5.9	5.2	5.6
Ol		2.6	3.8	2.1	tr	tr		
Cpx		0.3	1.0	7.3	1.5	1.3	1.2	0.5
Opx				0.2	tr	0.1	0.2	0.3
Mt		0.1	0.2	tr		0.2	0.6	
Pig					tr			
Σ phenos.		28.7	47.1	31.9	4.6	7.5	7.2	6.4
*Rheological properties**								
ρ magma	g/cm³	2.59	2.60	2.57	2.16	2.11	2.07	2.05
ρ plag	g/cm³	2.69	2.69	2.69	2.65	2.64	2.63	2.62
Log η	poise	3.3	3.1	3.4	3.8	4.5	5.1	5.5
Log V_s plag	m/s	−3.9	−3.8	−4.0	−4.4	−5.1	−5.6	−6.0
Log V_c plag	m/s	−4.7	−5.6	−4.9	−4.6	−5.3	−5.8	−6.2
$t_{1/2}$	yr	780	620	920	2620	13170	40120	102 210

Note: Compositional data are by XRF (Source: Singer et al., 1992a). Abbreviations: plag = plagioclase, ol = olivine, cpx = clinopyroxene, opx = orthopyroxene, mt = magnetite, pig = pigeonite, tr = trace amounts present.
* Rheological properties defined in the text.

1990). The often intricate plagioclase growth and dissolution histories facilitated by these techniques allow particularly detailed interpretations of magmatic processes (Anderson, 1984; Pearce et al., 1987b; Nixon and Pearce, 1987; Stamatelopoulou-Seymour et al., 1990; Pearce and Kolisnik, 1990; Kolisnik and Pearce, in preparation). Most detailed studies of plagioclase zoning have focused on arc volcanic systems, where open-system mixing of compositionally distinctive magmas is evident (e.g., Nixon and Pearce, 1987; Stamatelopoulou-Seymour et al., 1990; Sakuyama, 1981; Kawamoto, 1992; Halsor, 1989).

This study focuses on plagioclase zoning in mid-Pleistocene tholeiitic lavas, with compositions ranging from 49–71% SiO_2, erupted at the Seguam volcanic center, Aleutian arc, Alaska. Comprehensive petrologic and isotopic studies provide independent constraints on the evolution of these island arc lavas and have shown that they are related to one another through closed-system fractional crystallization (Singer et al., 1992a, 1992b, 1992c). Herein we present, for the first time, NDIC and NFLIM observations of plagioclase zoning patterns from a suite of arc lavas formed by closed-system fractional crystallization processes. It is our purpose to (1) characterize the textural and compositional complexity of plagioclase zoning in these lavas, (2) quantify the magnitude of oscillatory zoning and compositional shifts or discontinuities within plagioclase phenocrysts, (3) correlate where possible compositional shifts to intracrystalline structures or textures, and (4) use the zoning patterns with the in-

dependent petrologic evidence to illuminate the dynamic behavior of the magmas.

GEOLOGY, PETROGRAPHY, AND PETROLOGY

Seguam Island is a 205-km² central Aleutian volcanic center comprising ~80 km³ of mid-Pleistocene to Recent lava and pyroclastic flows (Singer et al., 1992a, 1992b). Unlike adjacent volcanic centers, Seguam grew atop extended arc crust (Singer and Myers, 1990); this local extensional environment is reflected in the unusual tholeiitic suite of low-K, high-Al basaltic and basaltic andesitic lavas and subordinate andesitic to rhyodacitic lavas. Lavas examined here (Table 1) represent the compositional and petrographic spectrum of the Turf Point Formation (TPF), which was formed 1.07–0.07 Ma. Basalts (49–52% SiO_2) and basaltic andesites (52–56% SiO_2) are crystal-rich, with 22–58% total phenocrysts dominated by plagioclase, and including olivine, augite, orthopyroxene (in basaltic andesites), and titanomagnetite. Andesites (56–63% SiO_2), dacites (63–68% SiO_2), and rhyodacites (68–71% SiO_2) are crystal-poor, with <8% total phenocrysts including plagioclase, augite, orthopyroxene, and titanomagnetite (Table 1).

In the basalts and basaltic andesites, plagioclase forms euhedral, tabular to equant phenocrysts 0.3–2.0 mm and, rarely, up to 5.0 mm long, with a variety of textures, including inclusion-free grains, crystals containing single or multiple inclusion-rich zones alternating with oscillatory zones and occasionally sieve-textured, glass inclu-

sion–rich cores. Phenocryst cores typically range from An_{70} to An_{93}, and most rims are between An_{50} and An_{80}. Plagioclase in the evolved lavas occurs as euhedral tabular or equant phenocrysts 0.3–2.0 mm long, with most cores between An_{45} and An_{70}. Several evolved lavas contain a small percentage of plagioclase phenocrysts with calcic ($An_{80–92}$) sieve-textured cores overgrown by sodic ($An_{40–70}$) inclusion-free zones. These crystal cores are interpreted as xenocrysts derived from basaltic precursors (see below). With the exception of these xenocrysts, plagioclase An content decreases systematically with increasing whole rock SiO_2. Nearly all the several hundred phenocrysts analyzed in 20 samples have thin rims (<50 μm) more sodic than the underlying cores (Singer et al., 1992a).

Whole rock major- and trace-element abundances vary along continuous trends of decreasing MgO, CaO, Al_2O_3, Cr, Ni, and Sr and increasing K_2O, Na_2O, Rb, Ba, Zr, Y, and Pb with increasing SiO_2. TiO_2 and Fe_{tot} (as FeO) vary along concave trends with SiO_2, as do the compatible elements Ni and Cr. REE abundances increase, and negative Eu anomalies become larger with increasing SiO_2 (Singer et al., 1992a). The TPF basaltic magmas were multiply saturated with plagioclase, olivine, clinopyroxene, and titanomagnetite at ~3–5 kbar, whereas andesitic to rhyodacitic magmas crystallized at lower pressure (Singer et al., 1992a). Preeruptive temperatures were 1150–1200 °C in the basalts and basaltic andesites and 900–1000 °C in the andesite to rhyodacite lavas (Singer et al., 1992a, 1992c).

Singer et al. (1992a) concluded that the basaltic andesites, andesites, dacites, and rhyodacites are related to a typical TPF basaltic parent magma by closed-system plagioclase-dominated fractional crystallization. This hypothesis is supported by successful major-element mass balance models, Rayleigh fractionation models of trace-element variation, and constant incompatible element and Sr, Nd, Pb, and O istotope ratios (Singer et al., 1992a, 1992c). Petrographic evidence of magma mixing or open-system behavior, such as reversely zoned plagioclase or pyroxene phenocrysts or resorbed xenocrysts, is absent. Repeated differentiation of small batches of basaltic parent magma during TPF volcanism at 1.07–0.07 Ma probably occurred in dikes fed from midcrustal chambers (Singer et al., 1992a). This contrasts with the adjacent calc-alkaline Aleutian volcanic centers, Adak and Kanaga, which are dominated by intermediate lavas (53–63% SiO_2), many preserving evidence of an open-system magma mixing origin (Conrad et al., 1983; Brophy, 1987, 1990).

ANALYTICAL METHODS

Polished sections of five basalts (49.7–52.0% SiO_2), two basaltic andesites (54.4 and 55.1% SiO_2), two andesites (58.3 and 62.7% SiO_2), one dacite (67.5% SiO_2), and one rhyodacite (71.0% SiO_2) that represent the spatial, temporal, textural, and geochemical range of TPF lavas were etched in fluoroboric acid, HBF_4, for 30–690 s. Zones

containing higher Ca contents are etched more deeply. The resulting microtopographic relief (≤0.5 μm) was enhanced utilizing reflected light NDIC microscopy (Anderson, 1983, 1984; Clark et al., 1986). Specimens were C coated to reduce internal reflections. Although the NDIC technique does not yield chemical composition directly, it dramatically improves the resolution of oscillatory zoning, sieve-textured zones, truncated zoning, and other features that may otherwise go unnoticed during routine petrographic or microprobe studies (Anderson, 1983; Pearce and Clark, 1989).

On the basis of optical and NDIC observations of several hundred crystals, representative phenocrysts from seven samples were analyzed using the NFLIM technique (Pearce, 1984a, 1984b) to obtain continuous zoning profiles. This study utilized blue-green light (516 nm) from a Spectra-Physics 164 Ar-ion laser. The source beam is expanded to a planar wave front; a beam splitter separates this light into a reference and sample beam. The beam passing through the sample becomes encoded with information concerning the distribution and magnitude of refractive index. Combination of the sample and reference beams produces an interference pattern or interferogram consisting of parallel light and dark fringes with displacements related to refractive index, hence, to composition. On the basis of the relations in Pearce (1984b), the distance between the dark fringes corresponds to a shift of 32 mol% An. The shift is precise to ±2 mol% An, with a spatial resolution of ~2–3 μm.

The laser interferograms were calibrated with the Cameca MBX microprobe at the University of Michigan. These analyses (Table 2) employed wavelength-dispersive measurements using a 15-kV accelerating potential, 20-nA beam current, 30-s counting time, and beam diameter of ~5 μm. Natural plagioclase standards were analyzed repeatedly to ensure accuracy. X-ray intensities were corrected for matrix effects using a modified Bence and Albee method (Albee and Ray, 1970).

OBSERVATIONS

Textural features: Optical and NDIC microscopy

TPF basalts and basaltic andesites contain plagioclase phenocrysts with texturally complex zoning patterns. Most commonly, these phenocrysts contain zones alternating between oscillatory euhedral and patchy, sieve-textured, or wavy morphologies (Fig. 1A–1E). Phenocryst cores typically show a weak, patchy, zoned morphology lacking abundant glass inclusions, although inclusion-rich and inclusion-free cores also occur (Fig. 1B, 1D). The patchy zones have little compositional heterogeneity and do not crosscut euhedral zones in the crystal cores (Fig. 1B, 1C). Sieve-textured zones 10–100 μm wide commonly form mantles on planar, locally fritted surfaces bounding oscillatory euhedral zones (Fig. 1A, 1C). The internal structure of the sieve-textured zones may rarely include disseminated submicrometer-sized melt inclusions (Fig. 1A) but is more commonly a coarse crystallographically or-

TABLE 2. Representative electron microprobe analyses of plagioclase in Turf Point Formation lavas

Sample Type Location	a J87-79 basalt Core	a J87-79 basalt Sieve	a J87-79 basalt Rim	b B87-9 bas. and. Core	b B87-9 bas. and. Rim	c B87-50 andesite Core	c B87-50 andesite Rim	d B87-67 dacite Core	d B87-67 dacite Rim	e B56 rhyodacite Core	e B56 rhyodacite Rim
SiO_2	44.2	46.5	45.8	47.1	48.4	47.2	51.9	53.2	54.4	57.3	58.4
Al_2O_3	34.5	33.3	33.4	33.2	31.7	32.5	29.4	28.3	28.0	26.5	25.4
FeO	0.56	0.71	0.75	0.71	0.80	0.79	0.78	0.65	0.03	0.38	0.33
CaO	18.9	17.4	17.7	16.9	15.6	16.3	12.62	11.4	10.7	8.47	7.75
Na_2O	0.91	1.72	1.54	1.89	2.75	2.15	4.15	4.96	5.31	6.64	7.05
K_2O	0.03	0.02	0.02	0.04	0.07	0.06	0.14	0.12	0.22	0.21	0.27
TOTAL	99.10	99.65	99.21	99.84	99.32	99.00	98.99	98.63	98.66	99.50	99.20
Mol% An	92	84	86	83	75	81	62	55	52	41	37

Note: a = phenocryst in Fig. 1C; b = phenocryst in Fig. 3A–3D; c = calcic-cored xenocryst in Fig. 3E–3H; d = phenocryst in Fig. 5A–5D; e = phenocryst in Fig. 5E–5H.

dered boxwork containing glass and fluid inclusions. In the coarse sieve-textured zones, partially devitrified glass inclusions 5–35 μm are spherical to elongate and commonly aligned subparallel to crystallographic axes (e.g., Figs. 1C, 2A, 3A). The fluid inclusions are typically spherical and <3–4 μm in diameter, and many contain liquid and vapor phases. The inclusions are concentrated near the flat, innermost boundaries of sieve-textured mantles and in concentric bands within sieve-textured zones (Fig. 4). Because of the high diffusivity of H_2O in feldspar, these inclusions probably contain CO_2-rich liquid and vapor (Roedder, 1984).

In the basalts and basaltic andesites, it is common to find two or more sieve-textured zones 10–100 μm wide separated by intervals of euhedral oscillatory zones 10–30 μm thick (Figs. 1A, 2A, 2B). Most phenocrysts are tabular and euhedral with oscillatory zoned rims 10–50 μm wide (Figs. 1B, 1C, 1D, 2). Depending on grain size, many phenocrysts in a particular sample share a common pattern of sieve-textured and euhedral oscillatory zones alternating inward from their rims (e.g., Fig. 1A–1D), suggesting a similar history. However, small populations of relatively simple or unusual crystals occur in these same

lavas, suggesting unique magmatic histories for some individual grains (Kolisnik and Pearce, in preparation).

Many basaltic andesite phenocrysts have the same alternating zoning pattern noted in the basalts. However, most also contain much simpler phenocrysts, with patchy zoned cores surrounded by a euhedral oscillatory zoned mantle. In sample B87-9, some phenocrysts have unusual irregular wavy zones (Fig. 1E), whereas others have anhedral embayed cores surrounded by sieve-textured glass and fluid inclusion–rich mantles (Fig. 3A–3D). The crossbedded pattern (Fig. 2F) and the highly convolute wavy zones (Fig. 1E) have not been previously reported.

TPF andesites, dacites, and rhyodacites contain two plagioclase phenocryst populations. One is characterized by simple fine-scale, ±2–4 mol% An, oscillatory zoning from core to rim (Fig. 1F–1H). Zone interfaces are planar and euhedral or gently curved, and typically they are conformable, not crosscutting. Less common are crystals with sieve-textured or patchy zoned calcic cores surrounded by more sodic mantles and rims (Fig. 3E, 3F). The cores of these phenocrysts are interpreted to be xenocrysts derived from parental basalts and basaltic andesites (see below). Excepting these xenocrysts, patchy or sieve-tex-

$\longrightarrow$

Fig. 1. NDIC images of etched plagioclase phenocrysts in Turf Point Formation lavas. (**A**) Portion of phenocryst in basalt J87-79. Note the patchy zoned An_{90} core with a planar, but fritted outer boundary (f) surrounded by a very fine sieve-textured mantle (m) that is, in turn, surrounded by a coarse-grained sieve-textured zone (s) with a thin An_{67} rim of narrow conformable oscillatory zones. Crosscutting nature of the fritted surface (f) and the texture of zone (m) suggest a reaction texture (Tsuchiyama, 1985). (**B**) Portion of phenocryst in basalt B87-57. Note the patchy zoned core mantled by euhedral oscillatory zones. Euhedral zones of the mantle are disturbed by a wavy zone 10 μm wide (wz), itself mantled by a conformable oscillatory zoned rim. (**C**) Phenocryst in basalt J87-79. This crystal lacks the fine sieve-textured mantle (m) as in **A** above, but has a similar core surrounded by a coarse sieve-textured zone and an oscillatory zoned rim. (**D**) Phenocryst in basalt B87-57 with similar texture to **B** above and illustrating that many features can be correlated

among phenocrysts from a single sample. (**E**) Phenocryst in basaltic andesite B87-9. The patchy zoned anhedral core may be resorbed along its margin, where it is surrounded by a mantle of complex wavy (wz) and fine sieve-textured zones (s) with a sodic rim. (**F**) Intergrown phenocrysts in andesite B87-49 showing low-amplitude euhedral oscillatory zoning from core to rim, unbroken by sieve-textured zones or dissolution surfaces and of a constant An_{70} composition. (**G**) Phenocryst in dacite B87-67 exhibits primarily euhedral oscillatory zoning as in **F** above, however, at least two unconformities are recognizable (arrows). Both are defined by curvilinear boundaries that truncate underlying planar euhedral zones. (**H**) Phenocryst in rhyodacite B87-56 shows fine-scale euhedral oscillatory zoning (2–3 μm) from core to rim. The inner core has a rounded boundary and rimward several zone interfaces are truncated and rounded (arrows). The crystal is zoned only from An_{55} to An_{52}.
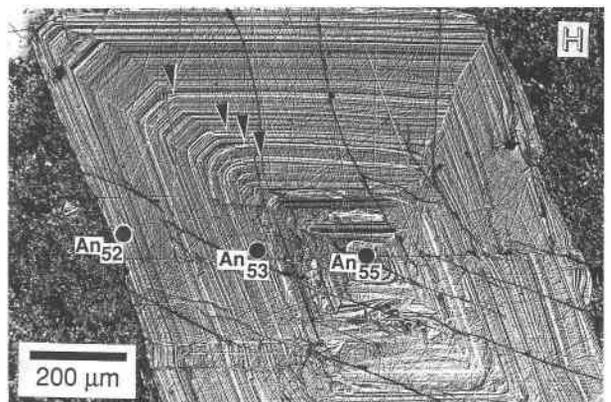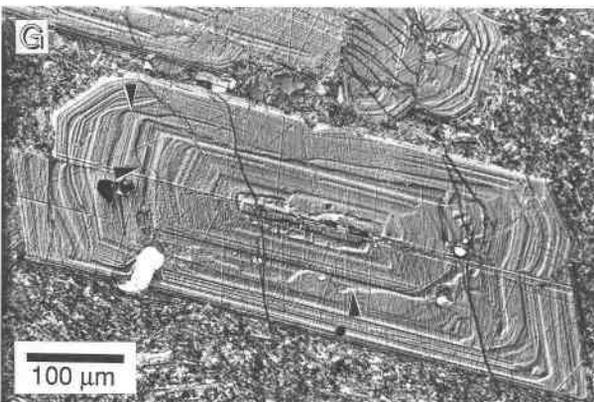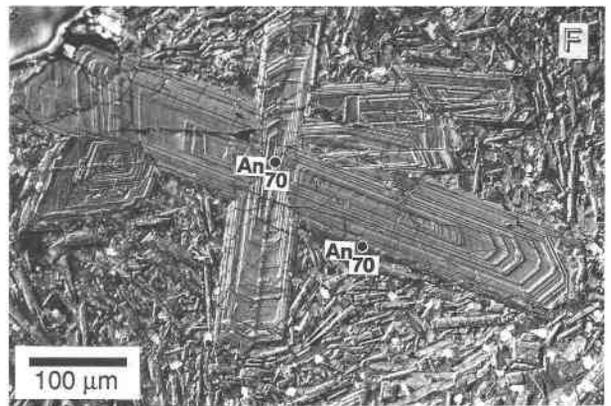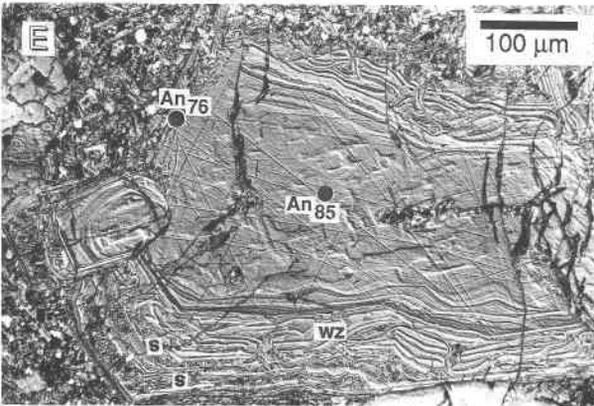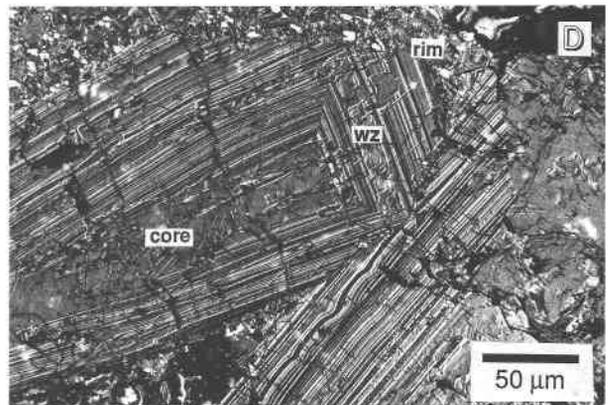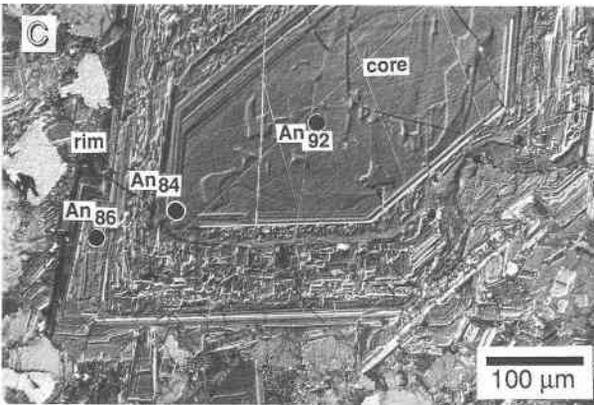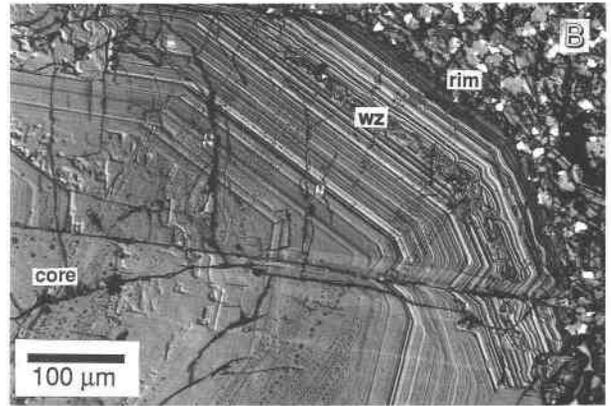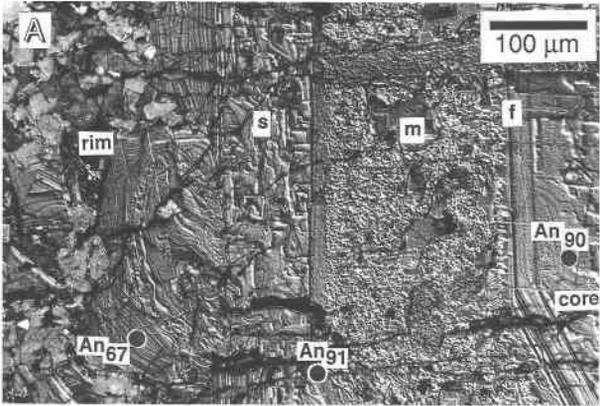
tured zones are absent, and fluid inclusions rarely occur. Resorption in the form of subtle rounding and truncation of phenocryst cores or initially euhedral oscillatory zones is, however, common (Fig. 1G, 1H). Up to five trunca-tions have been observed in some individual phenocrysts (Figs. 1H, 3F). These features are not readily detected using standard petrographic techniques (compare Fig. 3E, 3F).
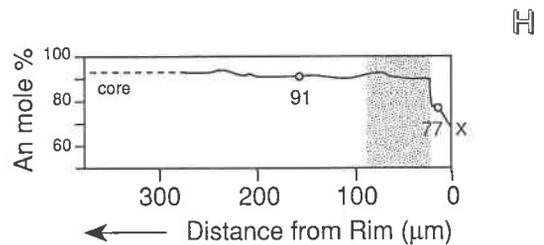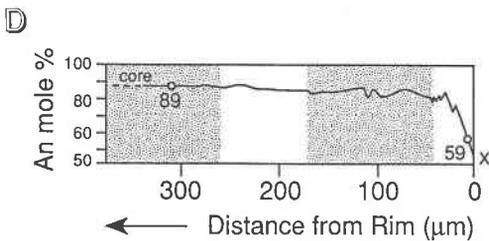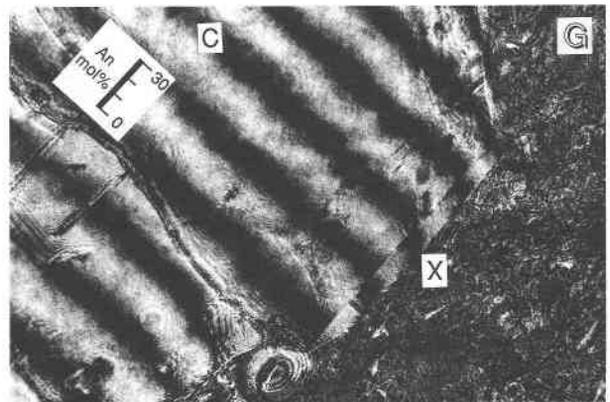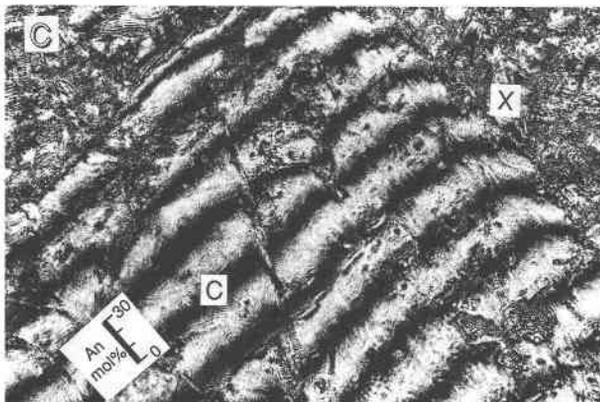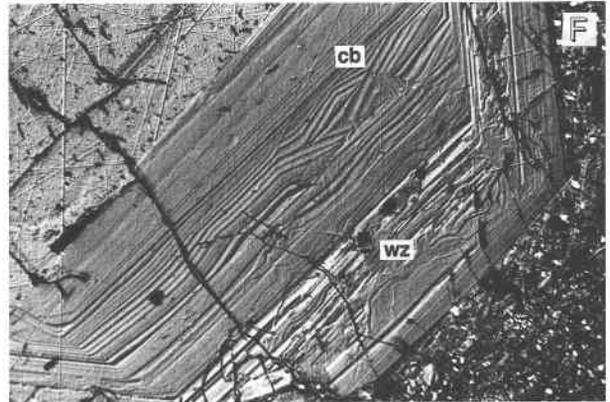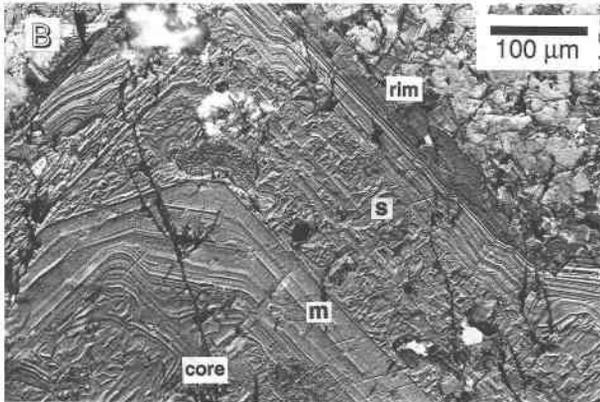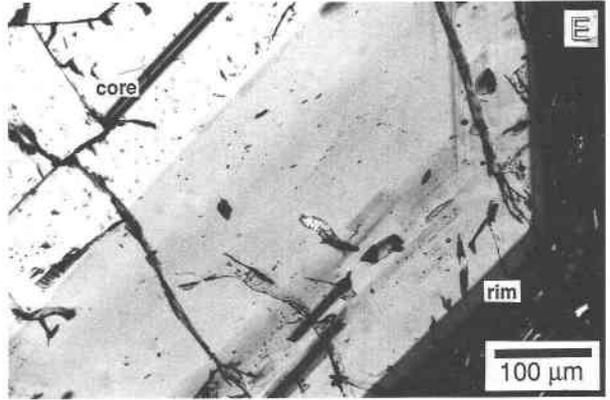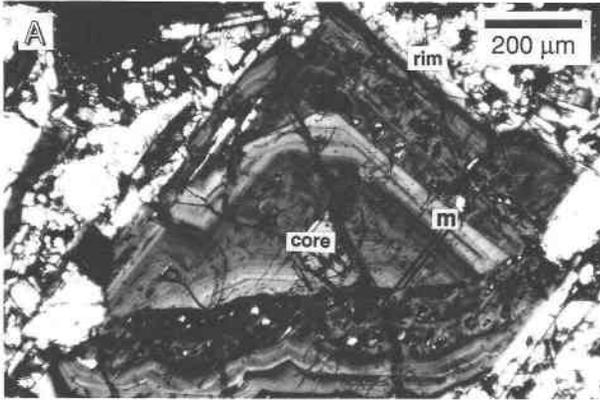
In contrast to the simple morphology of plagioclase in the more silicic TPF lavas, NDIC imaging of plagioclase phenocrysts in orogenic andesites and dacites from calc-alkaline volcanic centers in the Lesser Antilles, Cascades, Aegean arc, and Trans-Mexican Volcanic Belt reveals much more complex textural patterns, including multiple resorption surfaces and sieve-textured zones that clearly truncate and crosscut preexisting euhedral zones (Pearce et al., 1987b; Pearce and Kolisnik, 1990; Stamatelopoulou-Seymour et al., 1990; Kolisnik and Pearce, in preparation).

Laser interferometry: Zoning profiles and morphology

Despite the presence of sieve-textured glass and fluid inclusion–rich mantles surrounding phenocryst cores and alternations from sieve-textured to oscillatory zones, little, if any, variation in An content accompanies these features (Figs. 1A, 1B, 2A, 2B). Oscillations in the core and mantle regions of most phenocrysts are less than ± 2–3 mol% An, i.e., unresolvable with the NFLIM technique. All basaltic phenocrysts share the common trait of a thin rim, ≤ 50 μm, strongly zoned to more sodic compositions at the crystal-matrix interface (Fig. 2C, 2D, 2G, 2H). In most instances, the conformable zones comprising the rim are oscillatory (Fig. 2B, 2C, 2D). However, other crystals show an abrupt step to lower An content across sharp planar boundaries (Fig. 2G, 2H). Oscillations within the rim are typically on the order of ± 3–4 mol% An. Rim compositions correspond to those of groundmass plagioclase microlites, between An_{40} and An_{80} (Singer et al., 1992a). Differences between phenocryst cores and the crystal-matrix interface may be up to 35 mol% An (Fig. 2D, 2H).

Basaltic andesites share many of the same compositional features observed in the basalts, although the cores and rims are generally lower in An content. Despite clear evidence of resorption and inclusion-rich sieve-textured mantles, no compositional shifts accompany such changes (Fig. 3A–3D). Most phenocrysts in basaltic andesites are tabular and euhedral, and like those in the basalts, they commonly have normally zoned rims <50 μm thick, some

showing ~ 10-μm oscillations of up to 10 mol% An (Fig. 3C, 3D). Rare phenocrysts with resorbed anhedral cores have convolute zoned mantles up to to 10% lower in An content than the underlying core (Fig. 1E). The difference in composition between basaltic andesite phenocryst cores and the matrix interface in individual crystals is smaller than for the basalts, typically 15–20 mol% An (Fig. 3C, 3D). The range of compositions in the normally zoned phenocryst rims corresponds to that of groundmass microlites (Singer et al., 1992a).

Lavas of andesite to rhyodacite typically contain two populations of plagioclase phenocrysts with contrasting zoning profiles. One less abundant population consists of crystals with glass and fluid inclusion–rich sieve-textured cores of $>An_{80}$, commonly with subhedral to rounded forms, mantled by much more sodic euhedral oscillatory zones. For example, in Figure 3E–3G, there exists an abrupt step from a compositionally unzoned core of $\sim An_{80}$ to a mantle 30–110 μm wide that is reversely zoned from An_{67} to An_{78} in its outermost 10 μm. A zone <5 μm defines the rim, which is in some places skeletal, and records a shift from An_{78} to An_{62} at the crystal-matrix interface (Fig. 3H). The cores of this type of phenocryst are similar to portions of many plagioclases in the mafic lavas.

The predominant phenocryst population in the lavas of andesite to rhyodacite consists of euhedral tabular crystals with optically simple oscillatory euhedral zoning from core to rim (Figs. 5A, 5E). These oscillatory zones, 1–3 μm thick, may be interrupted at up to five concentric zone boundaries by subtle rounding and truncation of underlying zones (Fig. 1G, 1H). Regardless of morphology, these phenocrysts show only limited degrees of compositional zoning and become progressively more sodic with the increasing SiO_2 content of the host lava (Table 2). In dacite B87-67, oscillatory euhedral zones mantle an unzoned core of An_{55} that has an irregular shape (Fig. 5B, 5D). The oscillations are typically ± 5–10 mol% An. Although no unequivocal crosscutting or truncation of the oscillatory zones is observed, there exists a shift up to An_{60} and down to An_{45} within a zone 10 μm thick

---

$\leftarrow$

Fig. 2. Two examples of plagioclase zoning in TPF basalt. **(A)** Photomicrograph (cross-polarized light) of a mantled crystal fragment in basalt J87-79. **(B)** Close up NDIC image of the crystal in **A**. The core is an angular crystal fragment with a patchy zoned interior and euhedral oscillatory zoned margin (m). The fragment is surrounded by a coarse sieve-textured inclusion rich zone (s) with a flat inner boundary. This zone is surrounded by a euhedral oscillatory zoned rim 40 μm thick. **(C)** Narrow fringe laser interferogram of the crystal in **B**. Despite the textural variation, the fringe trace is nearly flat. Oscillatory zoning of ± 2–3 mol% An occurs in the euhedral rim, which shows a shift of >30 mol% An. **(D)** Digitized profile of the interferogram in **C** (traverse C = core to X = rim convention is followed here and in remaining profiles) showing An content as a function of distance from rim to core. Sieve-textured inclusion-rich or convolute zones

are shaded in this and succeeding profiles; open circles give An contents of spots calibrated by electron microprobe (Table 2). **(E)** Photomicrograph of portion of phenocryst in basalt B87-57. **(F)** NDIC image of same crystal in **E**. Fine irregularities, which resemble sedimentary cross bedding (cb), disrupt the oscillatory zoned mantle, which is surrounded by an irregular wavy zone (wz) with some inclusions and a euhedral oscillatory zoned rim. **(G)** Laser interferogram of crystal in **F** above. The core and mantle have a remarkably uniform composition; the only significant shift is an abrupt discontinuity of ~ 20 mol% An at the inner boundary of the rim. **(H)** Digitized profile of the interferogram in **G** above. The core, mantle, and convolute zone are all $An_{90 \pm 3}$. The abrupt step at the rim is from An_{90} to An_{77}, and the crystal margin is An_{68}.

surrounding the core, and the outermost 10 μm of this crystal is zoned from An_{53} to An_{40} (Fig. 5D). In contrast, a phenocryst in rhyodacite B87-56 differs from the previously described crystal. The core has a lower An content and is zoned from An_{41} to An_{34} where it is truncated by a rounded margin (Fig. 5F). Surrounding this truncated core boundary is a mantle of oscillatory euhedral zones 2 μm wide, but unlike the previous crystal, several of
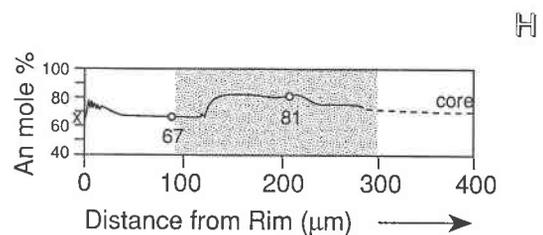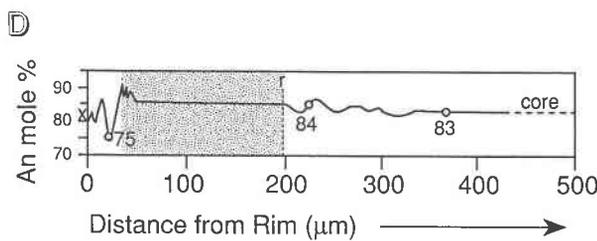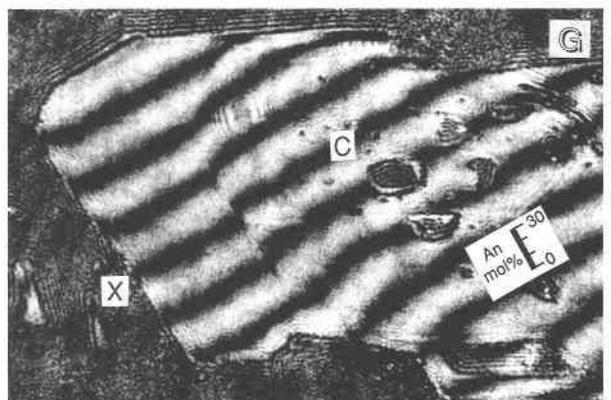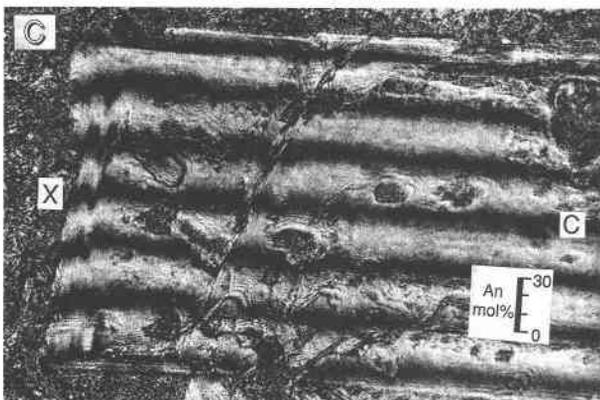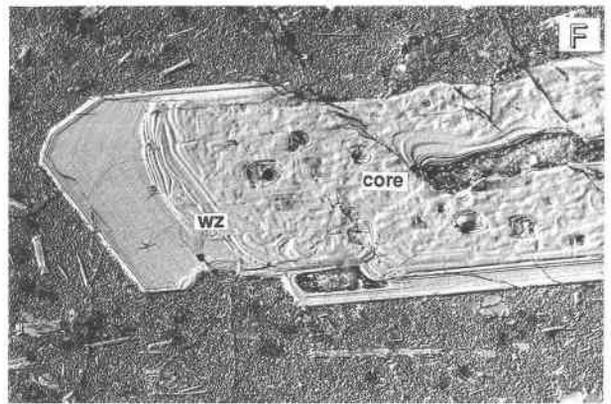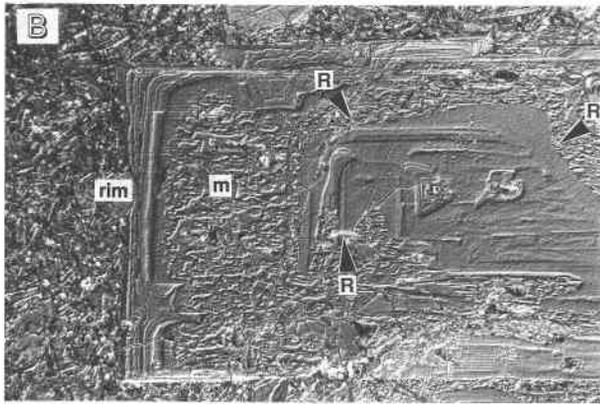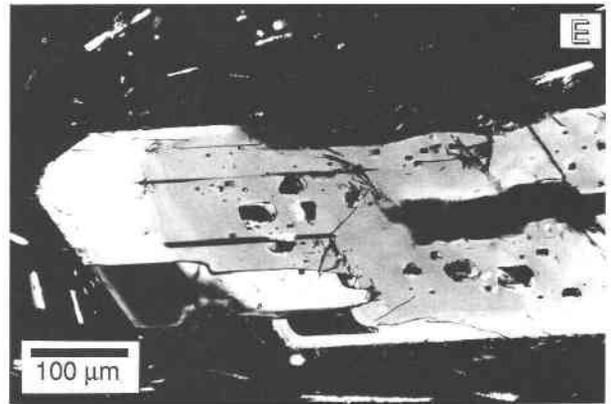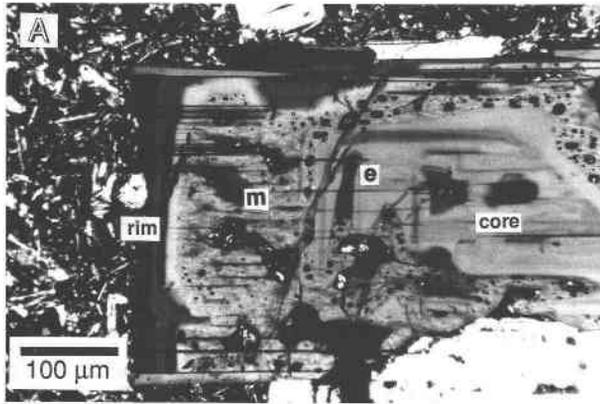
these zone interfaces are truncated (Fig. 5F). Rimward of each truncation surface occurs a ±4–6 mol% shift in An content (Fig. 5G, 5H). As with nearly all TPF crystals, there exists a euhedral zone several micrometers thick at the crystal margin, characterized by a drop in An content (Fig. 5H).

DISCUSSION

Basalts and basaltic andesites: The origin of sieve textures

The origin of sieve-textured or patchy zoned plagioclase has long been controversial (Kuno, 1950; Vance, 1965; MacDonald and Katsura, 1965; Dungan and Rhodes, 1978; Sakuyama, 1981; Kuo and Kirkpatrick, 1982; Anderson, 1984; Nelson and Montana, 1989, 1992). A common interpretation is that melt inclusions are trapped during the reaction between plagioclase and melt newly hybridized by magma mixing (MacDonald and Katsura, 1965; Dungan and Rhodes, 1978; Sakuyama, 1981; Halsor, 1989). However, changes in intensive parameters such as pressure or f_{H_2O} can also cause resorption or sieve-textured cellular growth of plagioclase (Vance, 1965; Wiebe, 1968; Pringle et al., 1974; Anderson, 1984; Nelson and Montana, 1989, 1992).

Tsuchiyama's (1985) dissolution experiments in the system Di-Ab-An produced dusty zones in sodic plagioclase immersed in melts saturated in higher temperature (more calcic) plagioclase. These dusty zones are calcic mantles riddled with a fine-grained and dense population of melt inclusions that surround unzoned, more sodic cores. Although these experiments produced textural and compositional patterns similar to those observed in arc lavas by MacDonald and Katsura (1965), Sakuyama (1981), and Kawamoto (1992) and seen only rarely in the TPF lavas (Fig. 1A), they failed to produce coarse melt
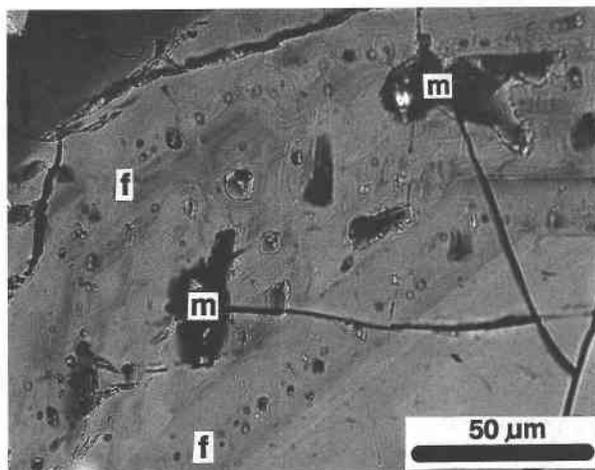
Fig. 4. Photomicrograph (500×; plane-polarized light) of details within a sieve-textured zone; same crystal as Fig. 1C. Note dark melt inclusions (m) up to 35 μm long and smaller translucent fluid inclusions 3–4 μm in diameter (f), some with trapped liquid and vapor bubbles. The fluid inclusions are concentrated in two zones (each labeled f) concentric about the unzoned core, which lies to the lower right.

inclusions like those typical of the TPF mafic lavas or MORBs. A magma mixing origin for melt inclusions in MORB is supported by a gridlike distribution of coarse inclusions along planes suggesting dissolution along intersecting cleavages and enclosure of sieve-textured cores by inclusion-free mantles with compositions differing from the cores by ±10 mol% An (Dungan and Rhodes, 1978). Kawamoto (1992) illustrates honeycomb plagioclase in a Japanese arc basalt with melt inclusions similar to those in TPF plagioclase. Abrupt drops of 10 mol% An outward from the melt inclusion–rich zones and the occur-

←

Fig. 3. Examples of plagioclase zoning in a TPF basaltic andesite (A–D) and andesite (E–H). (A) Photomicrograph (cross-polarized light) of portion of phenocryst in basaltic andesite B87-9. A coarse sieve-textured core is resorbed and mantled by a glass and fluid inclusion–riddled sieve-textured zone (m) that is surrounded by an oscillatory zoned rim. Note the deep glass filled embayment (e) crosscutting polysynthetic twins and planar zone boundaries in the core. (B) NDIC image of same crystal in A above. The resorption surface and embayments bounding the core are clearly evident (arrows labelled R). Surrounding this dissolution surface is a sieve-textured inclusion-rich zone (m) with a concentric alignment of inclusions surrounding the core. This zone is surrounded by a euhedral oscillatory zoned rim. (C) Narrow fringe laser interferogram of crystal in B. Despite the resorbed core and textural complexity, the crystal has a flat profile and an abrupt shift and oscillations of <10 mol% An confined to euhedral zones of the rim. (D) Digitized profile of the interferogram in C above. The core and mantle have a uniform composition of ~An_{83}. The exterior of the mantle, just outside the sieve-textured region, shows some fine oscillations of ±3% An and reverse zoning to An_{90}. There is an abrupt shift to An_{75}

at the inner boundary of the rim. The rim is oscillatory zoned and is An_{80} at the crystal-matrix interface. (E) Photomicrograph of portion of a phenocryst in andesite B87-50. The inclusion-rich core is overgrown by fine oscillatory euhedral zones extending to the rim. This crystal represents a less abundant population of xenocrystic plagioclase in andesites, dacites, and rhyodacites. More commonly, phenocrysts resemble those in Fig. 1F. (F) NDIC image of the same crystal in E above. The inclusion-riddled core is surrounded by an irregular wavy zone (wz) with a rounded outer termination. The outermost region of this crystal is a euhedral zone 80 μm thick with several delicate oscillations 2–3 μm wide. (G) Narrow fringe laser interferogram of the crystal in F above. The inclusion-rich core shows very limited shifts in composition of <±5% An content. There is an abrupt shift in composition of ~12 mol% An content at the outer termination of the wavy zone (wz). (H) Digitized profile of the interferogram in Fig. 1G. The mantle is reversely zoned from An_{67} to An_{78} between ~20 and 2 μm from the rim, but in the outermost 3–4 μm there is a shift from An_{78} to An_{65} at the crystal-matrix interface.

rence of dusty plagioclase in the same basalt suggest that the coarse melt inclusions were trapped by growth of plagioclase from melt supercooled by mixing with a more silicic magma (Kawamoto, 1992).

If the sieve-textured zones in TPF plagioclase were caused by dissolution rather than growth, Dungan and Rhodes (1978), Anderson (1984), and Pearce and Kolisnik (1990) suggest that critical tests are (1) zone bound-

aries of the preexisting crystal are truncated by the inclusions, and (2) inclusions should preferentially occur along lattice defects and energetically favorable surfaces (twin planes, etc.) parallel to crystallographic axes, resulting in a network of elongate channelways containing melt. The lack of compositional shifts associated with sieve-textured zones and the common absence of clear evidence of resorption (i.e., typically planar inner zone boundaries, no truncated relict euhedral zones, and no melt penetration along cleavages) favor cellular growth as the mechanism by which most of these zones formed in the TPF lavas. These same features are inconsistent with experimental and natural observations of plagioclase affected by the mixing of chemically and thermally distinct magmas.
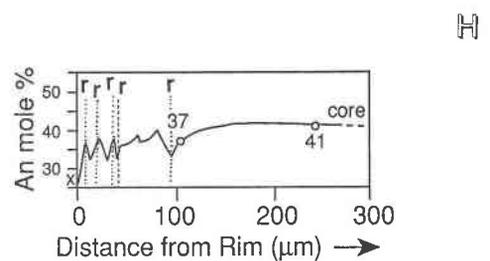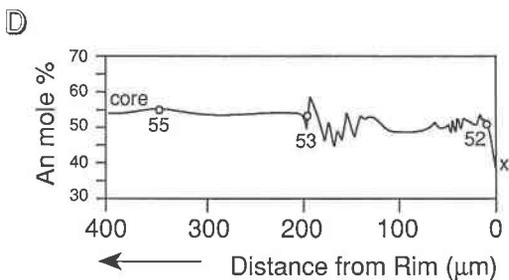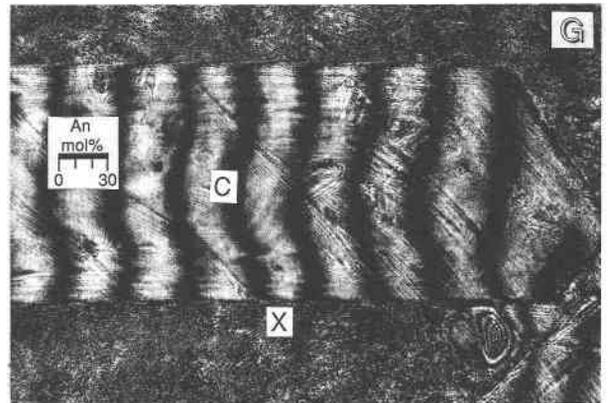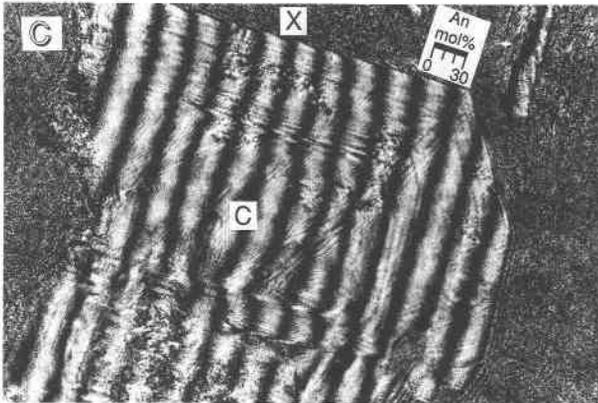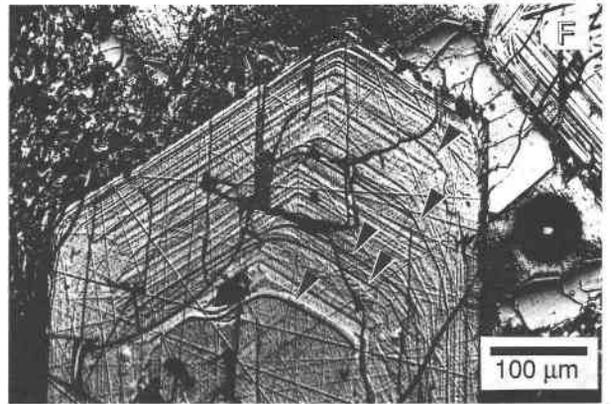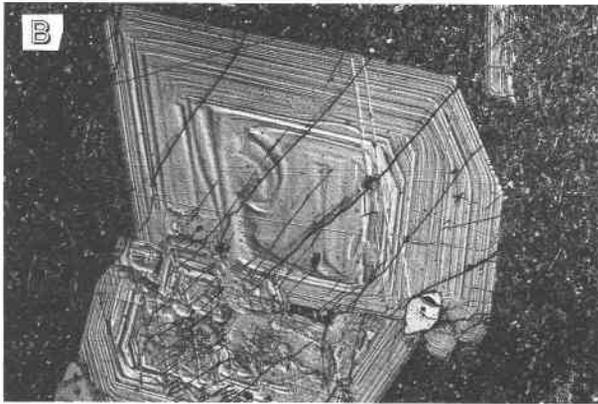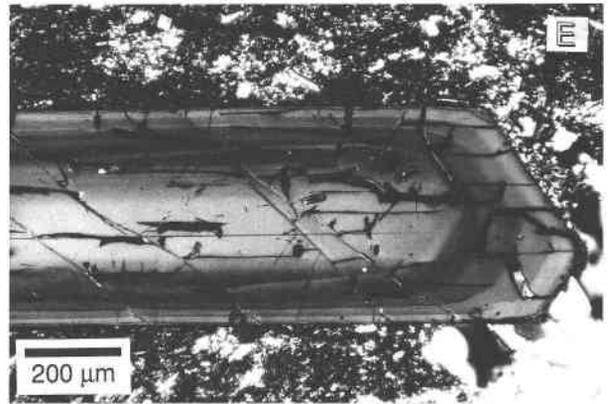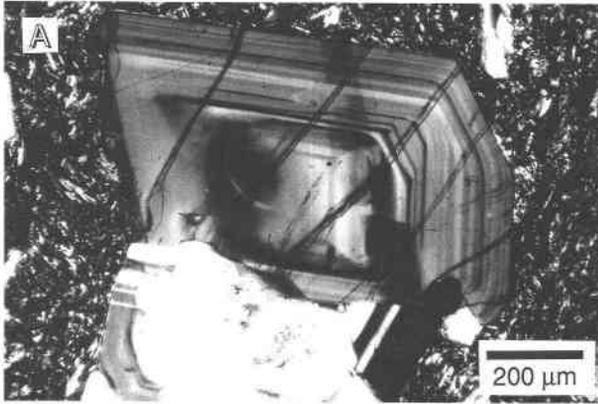
Isothermal decompression of anhydrous to moderately hydrous (undersaturated) magma lowers the plagioclase liquidus, increasing its An content (e.g., Vance, 1965; Loomis and Welber, 1982; Nelson and Montana, 1989). Nelson and Montana (1989, and personal communication, 1991) performed anhydrous isothermal decompression experiments on a plagioclase-phyric andesite that resulted in dissolution of plagioclase along channelways and that formed more extensive interconnected networks and coarse sievelike textures with increasing ΔP from 2 to 6 kbar. The resulting morphology resembles coarse-sieved textures in MORB plagioclase (Dungan and Rhodes, 1978; Kuo and Kirkpatrick, 1982) but not in the mantles of phenocrysts in TPF mafic lavas. Alternatively, decompression under vapor-saturated conditions is proposed to explain sodic sieve-textured zones surrounding slightly (<10 mol% An) more calcic oscillatory euhedral zones in plagioclase from basaltic andesite tephra erupted at Fuego volcano, Guatemala, in 1974 (Anderson, 1984).

Morphologically, the Fuego plagioclase represents a close analogue to that in mafic TPF lavas. Observations similar to those noted for the TPF crystals led Anderson (1984) to conclude that the sieve textures in Fuego plagioclase reflect "greater degrees of supersaturation and faster crystal growth than the oscillatory zoned portions of the phenocrysts" and not resorption due to magma mixing. Differences between the Fuego and TPF plagioclase are that no compositional shift is associated with most sieve-textured zones in the TPF mafic lavas and that in rare instances resorbed cores occur (Fig. 3A–3D).

We conclude that plagioclase zoning patterns in the TPF mafic lavas do not reflect mixing between compositionally distinctive magmas. The lack of reverse zoning of coexisting olivines and pyroxenes (Singer et al., 1992a) supports this conclusion. We propose instead that periods of relatively slow growth resulted in local boundary layer diffusion-controlled oscillatory euhedral zones, whereas sieve-textured inclusion-rich zones reflect trapping of melt and volatiles during rapid cellular growth, probably triggered by decompression-driven undercooling of some portion of the magma (e.g., Anderson, 1984). If so, the repetitive sieve-textured zones indicate that multiple decompression episodes affected most TPF mafic magmas. Decompression may correspond to pulses of wholesale magma ascent or rising limbs of convection cells in mafic magma chambers.

Admittedly, the resorbed and embayed cores of a few phenocrysts (Figs. 1E, 3A–3C) indicate that some plagioclase crystals experienced dissolution. This may reflect (1) more severe decompression of some crystals than others, (2) immersion in higher temperature magma, by either convective recycling (Blundy and Shimizu, 1991; Brophy, 1989; Marsh, 1989) or crystal settling (Martin and Nokes, 1989) in a thermally zoned magma chamber, or through magma mixing (Tsuchiyama, 1985), or (3) cumulate crystals from crystal-melt mushes along the walls and floors of the chamber. Convection of hot magma from the in-

←

Fig. 5. Examples of plagioclase zoning in Turf Point Formation dacites and rhyodacites. (A) Photomicrograph (cross-polarized light) of phenocryst in dacite B87-67. This crystal has an unzoned core surrounded by a mantle containing many fine oscillatory euhedral zones. (B) NDIC image of the same crystal reveals weak zoning in the core and at least 36 oscillatory zones averaging ~5 μm in width in the mantle. Although some zone interfaces are slightly rounded, no unequivocal evidence of truncation or dissolution is observed. (C) Narrow fringe laser interferogram of same crystal. The core is nearly uniform in composition; there is an abrupt transition to oscillatory zoning and compositional shifts of 10 and 14% An content in the innermost 15 μm of the mantle. There is a gradual shift in composition through the oscillatory zoned mantle over ~160 μm and a pronounced shift of 12% An content in the outermost 10 μm. (D) Digitized composition vs. distance profile for the same crystal. The core is An_{54-55}, except where it becomes slightly more sodic near its outer edge. The abrupt shift to oscillatory zoning at the core's edge corresponds to an increase in Ca content from An_{50} to An_{60} and a drop to An_{46} in the innermost 15 μm of the mantle. The magnitude of oscillations is <±8 mol% An in the outer part of the mantle, and there is a shift from An_{52} to An_{40} at the crystal-matrix interface. (E) Photomicrograph (cross-polarized light) of portion of phenocryst in rhyodacite B87-56. Several oscillatory zones can be seen in this tabular euhedral phenocryst. (F) NDIC image of the right end of the crystal in E above, magnified 2×. The core is unzoned and is rounded at its outer termination (arrow). Surrounding the core is a mantle consisting of numerous (>40) oscillatory euhedral zones. In at least four places, formerly euhedral zones are truncated and rounded (arrows). These subtle dissolution surfaces are not obvious with standard petrographic techniques (compare with A above). (G) Narrow fringe laser interferogram of the crystal in F above. The core is concentrically zoned with a smooth gradual shift of <10% An content from the center to edge. At the core's edge there is an abrupt shift in An content back to that of the core interior. Oscillatory zones of the mantle show shifts of ±5 mol% An. In the outer 10 μm, there is a drop of 10 mol% An. (H) Digitized profile of the interferogram in G above. The core is zoned from An_{41} to An_{33}. The oscillations in the mantle are within this range also. The outermost 10 μm is normally zoned from An_{36} to An_{26}. The locations of the dissolution surfaces identified in F above are shown as dashed lines labeled (r). These surfaces correspond to peaks in An content of the oscillatory zones in the mantle.
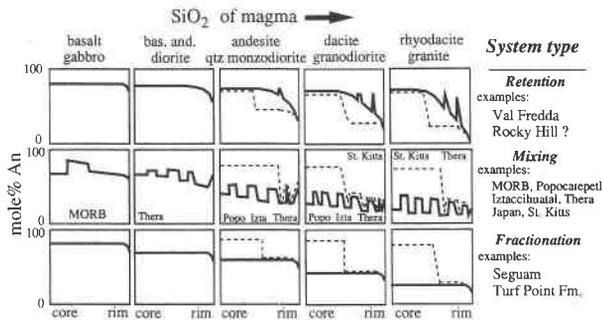
Fig. 6. Schematic illustration of gross features of plagioclase zoning profiles in three types of magmatic systems. Heavy lines indicate typical zoning patterns; lightly dashed lines illustrate profiles of less abundant xenocrysts characterized by pronounced compositional discontinuities. Although the mixing and fractionation dominated systems are well represented by volcanic examples, the retention-dominated type is based on less detailed zoning studies of calc-alkaline plutonic rocks (Blundy and Shimizu, 1991; Loomis and Welber, 1982). Other examples are from literature cited in the text.

terior of the chamber might shear and reentrain such crystals, resulting in resorption prior to renewed crystal growth (Blundy and Shimizu, 1991; Martin and Nokes, 1989). In any case, the lack of compositional zoning argues against extensive mixing of primitive and evolved mafic magmas.

We presently lack an explanation for the unusual highly convolute wavy or cross-bedded zoning in some calcic phenocrysts (Figs. 1E, 2F, 3F). A possible mechanism is growth during shearing at the melt-crystal interface.

Andesites, dacites, and rhyodacites: Origin of subtle dissolution

Truncation of euhedral oscillatory zone interfaces indicates that repeated episodes of dissolution punctuate the growth history of many phenocrysts. Whereas isothermal decompression experiments (ΔP of 2–6 kbar) did not produce simple dissolution of crystal surfaces (see above; Nelson and Montana, 1989, 1992), Tsuchiyama's (1985) and Lofgren and Norris's (1981) mixing experiments rapidly produced simple surface dissolution when sodic plagioclase was immersed in melts saturated with a higher temperature (more calcic) plagioclase. In systems where independent geochemical and mineralogical evidence suggests that magma mixing has been an important process, pronounced compositional shifts of 10–25% An content invariably accompany such dissolution surfaces (Nixon and Pearce, 1987; Stamatelopoulou-Seymour et al., 1990; Pearce and Kolisnik, 1990; Kolisnik and Pearce, in preparation; Kawamoto, 1992). In contrast, only very small compositional shifts, typically <5–10% An content, are associated with the truncated surfaces in plagioclase of the evolved TPF lavas, suggesting that extensive mixing of compositionally distinct magmas is an unlikely explanation for the truncations. The absence of reversely

zoned pyroxenes in the TPF lavas also argues against an important role for magma mixing (Singer et al., 1992a). It seems most likely that heating is responsible for the truncations in plagioclase of the silicic TPF lavas. If correct, these dissolution surfaces may reflect transport of the phenocrysts into hotter regions of a magma body, by convection of the magma or settling of crystals.

The calcic-cored xenocrysts (Fig. 3E–3H) record plagioclase nucleation and growth from basaltic melts, followed by resorption or a hiatus, then growth in cooler, more silicic melts. The cores of these crystals probably originated in mafic crystal-melt mushes along the walls of a magma chamber (e.g., Marsh, 1988, 1989; Martin and Nokes, 1989). These cumulates are complementary to extensive crystal fractionation from cooling basaltic magma that produced the andesites and dacites (Singer et al., 1992a). Convection or ascent of hotter magma within the interior of a chamber or dike shears the magma-mush zone interface and reentrains such phenocrysts (Martin and Nokes, 1989), resulting in some dissolution prior to renewed crystal growth. This mechanism has been suggested to explain remarkably similar plagioclase zoning profiles in the Val Fredda complex, Adamello, Italy (Blundy and Shimizu, 1991). The important conclusion is that bimodality of plagioclase core compositions does not necessitate mixing of compositionally distinctive liquids (e.g., dacites and basalts); rather, reentrainment of calcic cumulate plagioclase is envisioned to be a common process in magma chambers where extensive crystal fractionation occurs (Marsh, 1988, 1989; Martin and Nokes, 1989).

Other magmatic systems

Plagioclase zoning patterns in several other arc magmatic systems contrast with those in the TPF lavas. In the calc-alkaline Val Fredda gabbro to granite complex (Blundy and Shimizu, 1991) and the Rocky Hill zoned pluton, California (Loomis and Welber, 1982), many plagioclase crystals have smooth continuous zoning profiles punctuated by narrow calcic spikes. Phenocrysts in the Val Fredda complex all have cores of nearly identical composition that nucleated in the parental mafic endmembers. The more highly evolved rocks thus contain crystals showing extreme ranges in composition from core to rim that reflect protracted retention and growth in successively more evolved residual liquids (Fig. 6). The calcic spikes suggest retention and recycling of crystals through a compositionally zoned magma body (Blundy and Shimizu, 1991). Calcic-cored xenocrysts similar to those in the silicic TPF lavas are also common in the Val Fredda silicic rocks (Fig. 6) and suggest convection capable of reentraining cumulate crystals from chamber walls (Blundy and Shimizu, 1991).

Alternatively, plagioclase zoning in andesitic and dacitic lavas from many calc-alkaline volcanoes is commonly punctuated by multiple large amplitude shifts in composition (ΔAn of 10–25 mol%), corresponding to dissolution surfaces that reflect repetitive mixing of mafic and

silicic magmas or recycling of crystals through compositional gradients in strongly zoned magma chambers (Fig. 6; Nixon and Pearce, 1987; Pearce and Kolisnik, 1990; Stamatelopoulou-Seymour et al., 1990; Kolisnik and Pearce, in preparation; Sakuyama, 1981; Kawamoto, 1992). At Thera volcano, Greece, where a range of lava compositions has been affected by magma mixing, calcic-cored xenocrysts similar to those observed at Seguam and in the Val Fredda complex are also common (Fig. 6; Stamatelopoulou-Seymour et al., 1990) and may have a similar origin.

Plagioclase zoning and magma dynamics

Patterns of plagioclase zoning in the TPF lavas suggest that transport of magma and phenocrysts by convection, crystal settling, and magma ascent play important roles in the physical evolution of the TPF lavas. A sufficient body of theory exists to permit calculation of some basic dynamic properties of these magmas that may, in turn, illuminate in a qualitative sense processes consistent with the observed plagioclase zoning.

Martin and Nokes (1989) and Brophy (1989, 1991) showed that in thermally convecting magma chambers, middepth convective velocities nearly always exceed crystal settling velocities, and crystal retention is the rule. Martin and Nokes (1989) indicate, however, that adjacent to the chamber floor and walls, convective velocities diminish to zero at the boundary. In these boundary layers, crystal settling undoubtedly becomes an effective agent of magmatic differentiation (Martin and Nokes, 1989).

With the assumption of spherical crystals, the Stokes settling velocity in a crystal-free magma is given by

$$V_s = \frac{2\Delta\rho g a^2}{9\eta} \quad (1)$$

and in a crystal-rich magma Marsh and Maxey (1985) gave the crystal settling velocity as

$$V_c = V_s \langle (1 - N)/(1 + N^{\prime\prime}) \exp\{5N/3[1 - (N/N_m)]\} \rangle \quad (2)$$

where $\Delta\rho$ is the crystal-liquid density contrast, g is gravitational acceleration, a is the crystal radius, η is liquid viscosity, N is the volume fraction of suspended crystals, and N_m is the critical crystallinity in volume fraction (Marsh, 1981; Brophy, 1991), here given by 0.60.

Since V_c is an exponential function, the residence time of crystals that are retained in thermal convection and do not settle out of a convecting magma chamber can be expressed in terms of a half-life (Martin and Nokes, 1989):

$$t_{1/2} = (\ln 2)h(18\eta/g\Delta\rho a^2) \quad (3)$$

where h is the height of the magma chamber. Although the parameters above vary considerably during crystallization, the half-life gives a rough idea of rates of crystal fractionation and magmatic differentiation (Martin and Nokes, 1989; Blundy and Shimizu, 1991).

Taking the composition of TPF lavas (Table 1) to represent liquids unmodified by crystal sorting (Singer et al., 1992a, 1992b), we calculated anhydrous densities at 1100 °C and 1% H_2O (basalt and basaltic andesite) and 1000 °C and 2% H_2O (andesite–rhyodacite) from Lange and Carmichael's (1987) partial molar volume data corrected for H_2O using Burnham's (1979) H_2O solution model and the H_2O partial molar volume data of Burnham and Davis (1971). The densities of plagioclase at 1 atm (Deer et al., 1978) were corrected for thermal expansion (Skinner, 1966; compositions from Table 2). Liquid viscosities for the above conditions were calculated from Shaw (1972). Crystal radii of 1.0 mm (basalt and basaltic andesite) and 0.5 mm (andesite–rhyodacite) were assumed, based on typical TPF samples. These densities, viscosities, and crystal sizes were used in Equations 1, 2, and 3 to estimate crystal settling velocities and residence times in a magma chamber 1 km thick, assuming that the modal phenocryst abundances correspond to the volume fraction of suspended crystals (Table 1).

Calculated values of $\log \eta$ vary from 3.1–3.4 poise in the mafic lavas and to 3.8–5.5 poise in the silicic lavas (Table 1). Settling velocities are 600–100 m/yr in the mafic magmas and about 800–20 m/yr in the silicic magmas and concur with the range in values predicted by Brophy (1991). The half-life of plagioclase phenocrysts ranges from about 600 to 900 yr in the mafic lavas and 3000 to >100 000 yr in the silicic lavas. For comparison, values were also calculated using identical parameters for the presumed parental mafic magma (JM113) and a granodiorite composition (JM-155) of the Val Fredda complex (Fig. 6; Blundy and Shimizu, 1991). Log η, log V_c, and $t_{1/2}$ are 2.6 poise, −4.5 m/s (1000 m/yr), and 130 yr, in the mafic parent and 6.0 poise, −6.8 m/s (5 m/yr), and 700 000 yr in the granodiorite, respectively.

Two important results are, first, that the ranges of η, V_c, and $t_{1/2}$ values are similar, certainly within an order of magnitude, in the TPF and Val Fredda magma suites. The low values, <1000 yr, of $t_{1/2}$ for the mafic magmas are consistent with the conclusions of Martin and Nokes (1989) and Blundy and Shimizu (1991) that fractionation of basaltic magma must occur rapidly, on the order of a few thousand years, before solidification takes place (i.e., in six half-lives or ~6000 yr, 99% of a magma body 1 km thick will have crystallized and settled to form cumulates). Second, viscosity increases several orders of magnitude in the more silicic compositions (Table 1), which causes V_c to drop 2 orders of magnitude and $t_{1/2}$ values to increase 2 orders of magnitude. This is predicted by Martin and Nokes (1989) and indicates that plagioclase retention is strongly favored in more silicic magmas.

The hallmark of retention-dominated magma dynamics should be normally zoned plagioclase phenocrysts with large gradients from calcic cores to sodic rims (Fig. 6; Blundy and Shimizu, 1991). The flat zoning patterns of plagioclase in TPF magmas suggest that, in contrast to the Val Fredda complex (Fig. 6), plagioclase retention is

much less important in magma chambers beneath Seguam. Thus, despite the similarity in rheological properties, there exist pronounced differences in plagioclase zoning, and presumably magma dynamics, between Seguam and Val Fredda. If the small contrasts in rheological properties between these systems are insufficient to cause differences in the magma dynamics, then, as suggested by Brophy (1989, 1991), other external factors must be quite important. Foremost may be the wallrock-magma thermal contrast and the rate of magmatic cooling, which govern the thickness and therefore the volume of the convective boundary layer (Brophy, 1991; Martin and Nokes, 1989). Chamber size and geometry, eruption rates, and replenishment rates must also influence magma dynamics and differentiation processes (Marsh, 1989). For example, the TPF magmas crystallized at shallow crustal levels characterized by large wallrock-magma temperature contrasts and were readily erupted through fractured, extended arc crust (Singer and Myers, 1990; Singer et al., 1992a). Magma chamber boundary conditions in this environment favor rapid cooling, a thick convective boundary layer, and efficient crystal settling and fractionation. The flat plagioclase zoning patterns suggest that magma chambers are emptied frequently enough to preclude the long crystal residence times apparently necessary to form strongly zoned crystals. In contrast, the Val Fredda complex crystallized at a depth of about 4–5 km (Blundy and Shimizu, 1991), probably with slightly lower wallrock-magma thermal contrasts. This situation favored narrow convective boundary layers, less efficient crystal settling, and, since the intrusive complex could not readily erupt, convection remained vigorous and plagioclase retention was long-lived and widespread. The dynamics of either of these types of systems may be disrupted when the magma chambers are intercepted by new magma, or convective overturn causes mixing to occur. In systems where mixing is important, a third type of plagioclase zoning pattern is distinctive (Fig. 6).

The sieve-textured plagioclase in the mafic TPF lavas reflects episodic decompression during ascent of the magmas from relatively deep chambers. Were these crystals caught up in convective cycling, we suggest they would show more of a compositional gradient from core to rim than has been observed. As the Seguam magma systems evolved to more viscous silicic liquid compositions, plagioclase settling velocities declined and half-lives rose considerably. Because plagioclase retention was more likely in the silicic magmas, phenocrysts probably circulated repeatedly into hotter regions in the magma bodies, causing repetitive dissolution. However, the eruptive rate of TPF magmas was sufficiently high that phenocrysts traversed only a few convective cycles and show little compositional zoning in the lavas.

ACKNOWLEDGMENTS

REFERENCES CITED

Albee, A.L., and Ray, L. (1970) Correction factors for electron microanalysis of silicates, oxides, carbonates, phosphates, and sulphates. Analytical Chemistry, 42, 1408–1414.
Anderson, A.T. (1983) Oscillatory zoning of plagioclase: Nomarski interference contrast microscopy of etched polished sections. American Mineralogist, 68, 125–129.
———(1984) Probable relations between plagioclase zoning and magma dynamics, Fuego volcano, Guatemala. American Mineralogist, 69, 660–676.
Blundy, J.D., and Shimizu, N. (1991) Trace element evidence for plagioclase recycling in calc-alkaline magmas. Earth and Planetary Science Letters, 102, 178–197.
Brophy, J.G. (1987) The Cold Bay volcanic center, Aleutian volcanic arc. II. Implications for fractionation and mixing mechanisms in calc-alkaline andesite genesis. Contributions to Mineralogy and Petrology, 97, 378–388.
———(1989) Basalt convection and plagioclase retention: A model for the generation of high-alumina arc basalt. Journal of Geology, 97, 319–329.
———(1990) Andesites from northeastern Kanaga Island, Aleutians: Implications for calc-alkaline fractionation mechanisms and magma chamber development. Contributions to Mineralogy and Petrology, 104, 568–581.
———(1991) Composition gaps, critical crystallinity, and fractional crystallization in orogenic (calc-alkaline) magmatic systems. Contributions to Mineralogy and Petrology, 109, 173–182.
Burnham, C.W. (1979) The importance of volatile constituents. In H.S. Yoder, Ed., The evolution of the igneous rocks, fiftieth anniversary perspectives, p. 439–482. Princeton University Press, Princeton, New Jersey.
Burnham, C.W., and Davis, N.F. (1971) The role of H_2O in silicate melts. I. P-V-T relations in the system $NaAlSi_3O_8$-H_2O to 10 kilobars and 1000 °C. American Journal of Science, 270, 54–79.
Clark, A.H., Pearce, T.H., Roeder, P.L., and Wolfson, I. (1986) Oscillatory zoning and other microstructures in magmatic olivine and augite: Nomarski interference contrast observations on etched polished surfaces. American Mineralogist, 71, 734–741.
Conrad, W.K., Kay, S.M., and Kay, R.W. (1983) Magma mixing in the Aleutian arc: Evidence from cognate inclusions and composite xenoliths. Journal of Volcanology and Geothermal Research, 18, 279–295.
Deer, W.A., Howie, R.A., and Zussman, J. (1978) An introduction to the rock-forming minerals, 528 p. Longman, London.
Dungan, M.D., and Rhodes, J.M. (1978) Residual glasses and melt inclusions in basalts from DSDP legs 45 and 46: Evidence for magma mixing. Contributions to Mineralogy and Petrology, 67, 417–431.
Halsor, S.P. (1989) Large glass inclusions in plagioclase phenocrysts and their bearing on the origin of mixed andesitic lavas at Toliman Volcano, Guatemala. Bulletin of Volcanology, 51, 271–280.
Kawamoto, T. (1992) Dusty and honeycomb plagioclase: Indicators of processes in the Uchino stratified magma chamber, Izu peninsula, Japan. Journal of Volcanology and Geothermal Research, 49, 191–208.
Kuno, H. (1950) Petrology of Hakone volcano and the adjacent areas, Japan. Bulletin of the Geological Society of America, 61, 957–1020.
Kuo, L.C., and Kirkpatrick, R.J. (1982) Pre-eruption history of phyric basalts from DSDP legs 45 and 46: Evidence from morphology and zoning in plagioclase. Contributions to Mineralogy and Petrology, 79, 13–27.
Lange, R.L., and Carmichael, I.S.E. (1987) Densities of Na_2O-K_2O-CaO-MgO-FeO-Fe_2O_3-Al_2O_3-TiO_2-SiO_2 liquids: New measurements and derived partial molar quantities. Geochimica et Cosmochimica Acta, 51, 2931–2946.

Lofgren, G. (1974) Temperature induced zoning in synthetic plagioclase feldspar. In W.S. MacKenzie and J. Zussman, Eds., The feldspars, p. 363–373. Manchester University Press, Manchester, England.

Lofgren, G., and Norris, P.N. (1981) Experimental duplication of plagioclase sieve and overgrowth textures. Geological Society of America Abstracts with Programs, 13 (7), 498.

Loomis, T.P., and Welber, P.W. (1982) Crystallization processes in the Rocky Hill granodiorite pluton, California: An interpretation based on compositional zoning of plagioclase. Contributions to Mineralogy and Petrology, 81, 230–239.

MacDonald, G.A., and Katsura, T. (1965) Eruption of Lassen Peak, Cascade Range, California, in 1915: Example of mixed magmas. Geological Society of America Bulletin, 76, 475–482.

Marsh, B.D. (1981) On the crystallinity, probability of occurrence, and rheology of lava and magma. Contributions to Mineralogy and Petrology, 78, 85–98.

——— (1988) Crystal capture, sorting, and retention in convecting magma. Geological Society of America Bulletin, 100, 1720–1737.

——— (1989) Magma chambers. Annual Reviews of Earth and Planetary Science, 17, 439–474.

Marsh, B.D., and Maxey, M.R. (1985) On the distribution and separation of crystals in convecting magma. Journal of Volcanology and Geothermal Research, 24, 95–150.

Martin, D., and Nokes, R. (1989) A fluid-dynamical study of crystal settling in convecting magma. Journal of Petrology, 30, 1471–1500.

Nelson, S.T., and Montana, A. (1989) Plagioclase resorption textures as a consequence of the rapid isothermal decompression of magmas. IAVCEI abstracts, New Mexico Bureau of Mines and Mineral Resources Bulletin, 131, 202 p.

——— (1992) Sieve-textured plagioclase in volcanic rocks produced by rapid decompression. American Mineralogist, 77, 1242–1249.

Nixon, G.T., and Pearce, T.H. (1987) Laser-interferometry study of oscillatory zoning in plagioclase: The record of magma mixing and phenocryst recycling in calc-alkaline magma chambers, Iztaccihuatl volcano, Mexico. American Mineralogist, 72, 1144–1162.

Pearce, T.H. (1984a) Multiple frequency laser interference microscopy: A new technique. The Microscope, 32, 69–81.

——— (1984b) Optical dispersion and zoning in magmatic plagioclase: Laser-interference observations. Canadian Mineralogist, 22, 383–390.

Pearce, T.H., and Clark, A.H. (1989) Nomarski interference contrast observations of textural details in volcanic rocks. Geology, 17, 757–759.

Pearce, T.H., and Kolisnik, A.M. (1990) Observations of plagioclase zoning using interference imaging. Earth-Science Reviews, 29, 9–26.

Pearce, T.H., Griffin, M.P., and Kolisnik, A.M. (1987a) Magmatic crystal stratigraphy and constraints on magma chamber dynamics: Laser interference results on individual phenocrysts. Journal of Geophysical Research, 92, 13745–13752.

Pearce, T.H., Russell, J.K., and Wolfson, I. (1987b) Laser interference and Nomarski interference imaging of zoning profiles in plagioclase phenocrysts from the May 18, 1980, eruption of Mount St. Helens, Washington. American Mineralogist, 72, 1131–1143.

Pringle, G.J., Trembath, L.T., and Parjari, G.E., Jr. (1974) Crystallization history of a zoned plagioclase. Mineralogical Magazine, 39, 867–877.

Roedder, E. (1984) Fluid inclusions. Mineralogical Society of America Reviews in Mineralogy, 12, 644 p.

Sakuyama, M. (1981) Petrological study of the Myoko and Kurohima volcanos, Japan: Crystallization sequence and evidence for magma mixing. Journal of Petrology, 22, 553–583.

Shaw, H.R. (1972) Viscosities of magmatic silicate liquids, an empirical method of prediction. American Journal of Science, 272, 870–893.

Singer, B.S., and Myers, J.D. (1990) Intra-arc extension and magmatic evolution in the central Aleutian arc, Alaska. Geology, 18, 1050–1053.

Singer, B.S., Myers, J.D., and Frost, C.D. (1992a) Mid-Pleistocene lavas from the Seguam volcanic center, central Aleutian arc, Alaska: Closed system fractional crystallization of a basalt to rhyodacite eruptive suite. Contributions to Mineralogy and Petrology, 110, 87–112.

——— (1992b) Mid-Pleistocene basalt from the Seguam volcanic center, central Aleutian arc, Alaska: Local lithospheric structures and source variability in the Aleutian arc. Journal of Geophysical Research, 97, 4561–4578.

Singer, B.S., O'Neil, J.R., and Brophy, J.G. (1992c) Oxygen isotope constraints on the petrogenesis of Aleutian arc magmas. Geology, 20, 367–370.

Skinner, B.J. (1966) Thermal expansion. Geological Society of America Memoir, 97, 25–28.

Stamatelopoulou-Seymour, K., Vlassopoulos, D., Pearce, T.H., and Rice, C. (1990) The record of magma chamber processes in plagioclase phenocrysts at Thera volcano, Aegean volcanic arc, Greece. Contributions to Mineralogy and Petrology, 104, 73–84.

Tsuchiyama, A. (1985) Dissolution kinetics of plagioclase in the melt of the system diopside-albite-anorthite, and the origin of dusty plagioclase in andesites. Contributions to Mineralogy and Petrology, 89, 1–16.

Vance, J.A. (1965) Zoning in igneous plagioclase: Patchy zoning. Journal of Geology, 73, 636–651.

Wiebe, R.A. (1968) Plagioclase stratigraphy: A record of magmatic conditions and events in a granitic stock. American Journal of Science, 266, 690–703.